

# Ion Activities in Dilute Solutions near the Critical Point of Water

Jason A. Myers\* and Stanley I. Sandler

Department of Chemical Engineering, University of Delaware, Newark, Delaware 19716

Robert H. Wood and Victor N. Balashov

Department of Chemistry and Biochemistry, University of Delaware, Newark, Delaware 19716

Received: April 19, 2003; In Final Form: July 14, 2003

The mean ionic activity coefficients of dilute electrolyte solutions show large anomalies near the critical point of water. Activity coefficients of aqueous NaCl solutions were calculated with an electrolyte equation of state at several different near-critical temperatures and densities. At the critical point, the activity coefficients are proportional to  $x^{1/3}$ , where  $x$  is the mole fraction of solute, which is consistent with a classical expansion of the Helmholtz free energy near the critical point. At all points, except exactly at the critical point, the Debye–Hückel limiting law is valid in a range that diminishes as the critical point is approached; also vestiges of the  $x^{1/3}$  limiting law appear at higher concentrations. For ions, large (50%) anomalies in the activity coefficients of 0.01 *m* NaCl solutions are seen at up to 100 °C above the critical temperature and 0.2 g/cm<sup>3</sup> above the critical density. In the present model, these anomalies are large for ions because of significant electrostriction that increases the dielectric constant of water. The electrical conductance measurements on NaCl near the critical point of water indicate that the present model may overestimate the anomalous effect.

## Introduction

It is well known that the activity coefficients of dilute aqueous solutions exhibit large anomalies along the critical isotherm–isobar.<sup>1–3</sup> For electrolyte solutions, the Debye–Hückel limiting law<sup>4</sup> is no longer valid on the critical isotherm–isobar. Instead, for classical systems, there is a  $x^{1/3}$  limiting law, and for nonclassical systems, there is a  $x^{1/\delta}$  law where  $\delta = 4.815$  and  $x$  is the mole fraction of solute.

Levelt Sengers et al.<sup>1</sup> pointed out that, “On any other isotherm–isobar, a vestige of this critical behavior will remain, in the sense that regular behavior will compete with the critical effect, and assert itself more strongly, and in a larger  $x$  range starting at  $x = 0$ , as the fluid is removed from  $P_c$ ,  $T_c$ .” The importance of these vestiges near the critical point has been recognized<sup>1–3,5</sup> and the anomalous effects on heat capacities and volumes have been studied,<sup>6–13</sup> but to our knowledge there is no study of the effects on activity coefficients. Consequently, the range of temperature and density over which there are significant effects on the activity coefficients is unknown. Gruszkiewicz and Wood<sup>14</sup> found that the usual equilibrium treatment with Debye–Hückel limiting law activity coefficients was sufficient to fit their conductance data 2.5 K above the critical point and at the critical density and suggested that their data provided no evidence for the existence of these vestiges. The purpose of this paper is to explore the ranges over which these vestiges are significant using the recent classical equation of state of Myers et al.<sup>15</sup> Because this is a classical equation of state, it will have classical exponents. Because the equation of state was parametrized only up to 300 °C, the results we obtain will be only semiquantitative. However, we believe that the range and magnitude of the effects will be similar to those for real solutions, so the calculations here should provide a useful

guide as to where these effects can be expected. We should also note that the equation of state of Myers et al. is valid for solutions of ions and solvent only. At high temperatures, such as those encountered near the critical point, there will be significant ion pairing, especially in highly concentrated salt solutions. However, in this work we are interested only in the critical-point behavior of dilute ions; therefore, we do not take into account any ion pairing that may occur.

## Electrolyte Solution Model

The equation of state of Myers et al.<sup>15</sup> is an expression for the Helmholtz free energy as a function of temperature, volume, and number of moles of each component in the solution and is given as the sum of three terms:

$$A(T, V, \mathbf{n}) - A^{\text{IGM}}(T, V, \mathbf{n}) = \Delta A^{\text{PR}} + \Delta A^{\text{Born}} + \Delta A^{\text{MSA}} \quad (1)$$

$T$  is the temperature of the system,  $V$  is the system volume,  $\mathbf{n}$  is the vector of the number of moles of each component of the mixture, and  $A^{\text{IGM}}$  is the Helmholtz free energy of an ideal gas mixture. The individual parts of the model will be briefly described here.

The first part of the equation of state is the Peng–Robinson contribution, which accounts for the short-range interactions between all species in solution. The residual Helmholtz free energy for the volume-translated Peng–Robinson equation of state is

$$\Delta A^{\text{PR}}(T, V, \mathbf{n}) = \frac{N \cdot a}{2\sqrt{2}b} \ln \left[ \frac{V + c + b(1 - \sqrt{2})}{V + c + b(1 + \sqrt{2})} \right] - NRT \ln \left( \frac{V + c - b}{V} \right) \quad (2)$$

where  $a$  is the van der Waals attraction parameter,  $b$  is the van

\* To whom correspondence should be addressed. E-mail: myersja@che.udel.edu. Phone: (302) 831-0875. Fax: (302) 831-3226.

der Waals excluded volume parameter,  $c$  is the volume translation parameter,  $V$  is the molar volume,  $N$  is the total number of moles, and  $R$  is the gas constant. The  $a$ ,  $b$ , and  $c$  parameters in eq 2 are specific to the mixture and can be calculated from the pure-component parameters with the van der Waals one-fluid mixing rules:

$$a = \frac{1}{N^2} \sum_i \sum_j n_i n_j \sqrt{a_i a_j} (1 - k_{ij}) \quad (3)$$

$$b = \frac{1}{N} \sum_i n_i b_i \quad (4)$$

$$c = \frac{1}{N} \sum_i n_i c_i \quad (5)$$

$a_i$ ,  $b_i$ , and  $c_i$  are the pure-component van der Waals attraction parameter, excluded volume parameter, and volume translation parameter, respectively, and  $k_{ij}$  is a binary interaction parameter. The volume translation parameter added to the original Peng–Robinson equation greatly improves density predictions, especially near the critical point where cubic equations of state often fail to predict densities accurately.

The second part of the equation of state is the Born contribution, which accounts for the change in Helmholtz free energy on discharging ions in a vacuum and recharging in a dielectric solvent. The change in Helmholtz free energy for this contribution is given by

$$\Delta A^{\text{Born}}(T, V, \vec{n}) = -\frac{N_a e^2}{4\pi\epsilon_0} \left(1 - \frac{1}{\epsilon}\right) \cdot \sum_{\text{ions}} \frac{n_i Z_i^2}{\sigma_i} \quad (6)$$

where  $N_a$  is Avogadro's number,  $e$  is the unit of elementary charge,  $\epsilon_0$  is the permittivity of free space,  $\epsilon$  is the dielectric constant,  $Z_i$  is the charge number of ion  $i$ , and  $\sigma_i$  is the ion diameter. The dielectric constant used here is that of the pure solvent (water) calculated from the model of Uematsu and Franck.<sup>16</sup> If desired, the more accurate dielectric constant correlation of Fernandez et al.<sup>17</sup> can be used, although the equation-of-state parameters would need to be refit. Our results do not significantly differ between the two models, and we have chosen to use the Uematsu and Franck model in our calculations here.

The third part of the equation of state is the mean spherical approximation (MSA) contribution that accounts for the long-range charge–charge interactions between ions. Here we use a simple approximation to the MSA derived by Harvey et al.<sup>18</sup> in which all ions are modeled as charged hard spheres with a single average diameter given by

$$\sigma = \frac{\sum_{\text{ions}} n_i Z_i^2 \sigma_i}{\sum_{\text{ions}} n_i Z_i^2} \quad (7)$$

The MSA contribution to the Helmholtz free energy of the system is

$$\Delta A^{\text{MSA}}(T, V, \vec{n}) = -\frac{2\Gamma^3 RTV}{3\pi N_a} \left(1 + \frac{3}{2}\sigma\Gamma\right) \quad (8)$$

where  $\Gamma$  is the MSA screening parameter and  $\kappa$  is the Debye screening length. These quantities are

$$\Gamma = \frac{1}{2\sigma} [\sqrt{1 + 2\sigma\kappa} - 1] \quad (9)$$

and

$$\kappa = \left( \frac{e^2 N_a^2}{\epsilon \epsilon_0 RTV} \sum_{\text{ions}} n_i Z_i^2 \right)^{1/2} \quad (10)$$

It is important to note that the MSA equation reduces to the Debye–Hückel limiting law as  $\sigma$  approaches zero and as the ionic concentrations approach zero; however, the MSA equation gives much more accurate predictions of the thermodynamic properties at high electrolyte concentrations.

The electrolyte equation of state has three parameters for each solvent species ( $a$ ,  $b$ , and  $c$ ) and four parameters for each ionic species ( $a$ ,  $b$ ,  $k_{\text{ion-water}}$ , and  $\sigma$ ). For water, the following parameter set was used:

$$a_{\text{H}_2\text{O}} = 1.26944 - 0.89381 \cdot T_r + 0.16937 \cdot T_r^2 \text{ Pa m}^6/\text{mol} \quad (11)$$

$$b_{\text{H}_2\text{O}} = 15.6345 + 6.14518 \cdot T_r - 5.2795 \cdot T_r^2 \text{ cm}^3/\text{mol} \quad (12)$$

$$c_{\text{H}_2\text{O}} = -2.7227 + 11.4201 \cdot T_r - 6.0157 \cdot T_r^2 \text{ cm}^3/\text{mol} \quad (13)$$

where  $T_r = T/647.29$  K. For NaCl, the following parameter set was used:

$$a_{\text{Na}^+} = a_{\text{Cl}^-} = 0.932 - \frac{207.9}{T} \text{ Pa m}^6/\text{mol} \quad (14)$$

$$b_{\text{Na}^+} = b_{\text{Cl}^-} = 9.90 \text{ cm}^3/\text{mol} \quad (15)$$

$$k_{\text{Na}^+-\text{water}} = k_{\text{Cl}^--\text{water}} = -0.2540 \quad (16)$$

$$\sigma_{\text{Na}^+} = \sigma_{\text{Cl}^-} = 5.695 - \frac{551.3}{T} \text{ \AA} \quad (17)$$

Table 1 gives the critical properties of water calculated from the equation of state as well as the experimental values.<sup>19</sup> Although the equation of state slightly overpredicts the critical temperature and pressure, this is not of importance when investigating the behavior of activity coefficients of a dilute solute near the critical point. In our calculations, to be consistent, we use the values of the critical properties predicted from the equation of state instead of the experimental values because it is the equation-of-state behavior that we are interested in. Therefore, when we mention the critical temperature and density of water, we are referring to the equation-of-state values in Table 1.

## Activity Coefficients

Because we have developed a Helmholtz free energy model for electrolyte solutions, any thermodynamic property of the system can be calculated from its various temperature, volume, and mole number derivatives. Of primary importance in this work are the activity coefficients of the ionic species. For dilute species such as electrolytes, the activity coefficients are reported in the hypothetical ideal 1  $m$  standard state. These activity coefficients are defined by the following relation:

$$\mu_i = \mu_i^m + RT \ln(m_i \gamma_i^m) \quad (18)$$

**TABLE 1: Experimental and Equation-of-State Predictions of the Critical Properties of Pure Water**

	critical temperature (K)	critical pressure (MPa)	critical density (g/cm <sup>3</sup> )
experimental <sup>19</sup>	647.096	22.064	0.322
equation of state	663.43	26.188	0.290

$\mu_i$  is the chemical potential of species  $i$ ,  $m_i$  is the molality of species  $i$  in mol/kg,  $\gamma_i^m$  is the molality-based activity coefficient, and  $\mu_i^m$  is the chemical potential of a hypothetical ideal 1  $m$  solution of species  $i$ , which can be calculated from

$$\mu_i^m = \lim_{m_i \rightarrow 0} (\mu_i - RT \ln m_i) \quad (19)$$

The chemical potential of any component can be calculated from the equation of state using

$$\mu_i = \left( \frac{\partial A}{\partial n_i} \right)_{T,V,n_{j \neq i}} \quad (20)$$

The mean ionic activity coefficient can then be calculated from the equation of state using

$$\ln \gamma_i^m = \frac{\mu_i}{RT} - \ln m_i - \lim_{m_i \rightarrow 0} \left( \frac{\mu_i}{RT} - \ln m_i \right) \quad (21)$$

and

$$\gamma_{\pm}^m = [(\gamma_+^m)^{\nu_+} (\gamma_-^m)^{\nu_-}]^{1/\nu} \quad (22)$$

where  $\nu_+$  and  $\nu_-$  are the number of cations and anions, respectively, in one molecule of the salt and  $\nu$  is the total number of molecules upon complete dissociation of one molecule of salt.

### Calculations

Levelt Sengers<sup>3</sup> and Chang and Levelt Sengers<sup>20</sup> used classical theory and expanded the Helmholtz free energy of a dilute nonionic mixture around the critical point of the solvent in terms temperature, volume, and mole fraction of solute to obtain expressions for the infinite dilution thermodynamic properties of the solute. They found that, near the critical point, the activity coefficient of a dilute solute is proportional to  $x^{1/3}$ . For dilute ionic solutions, the Debye–Hückel model predicts an activity coefficient proportional to  $x^{1/2}$ . Thus, we would like to determine where the Debye–Hückel law is valid and in what region near the critical point of water the  $x^{1/3}$  behavior occurs for electrolyte solutions.

To do this, we first calculated the mean ionic activity coefficient of NaCl as a function of salt molality ( $m$ ) at the critical point. We then calculated activity coefficients as functions of  $m$  at  $T = T_c + \delta T_c$  and  $\rho_0 = \rho_c + \delta \rho_c$  along paths of constant pressure for several different values of  $\delta T_c$  and  $\delta \rho_c$ . Our results are plotted in Figures 1 and 2 along with the activity coefficients predicted by the MSA. We should note that at the low concentrations studied here the MSA and Debye–Hückel activity coefficients are approximately equal because the MSA reduces to the Debye–Hückel limiting law as  $m$  approaches zero. The dashed lines in these Figures will be discussed later.

### Discussion

Our results in Figures 1 and 2 indicate that the Debye–Hückel limiting law is valid at all state points except on the critical

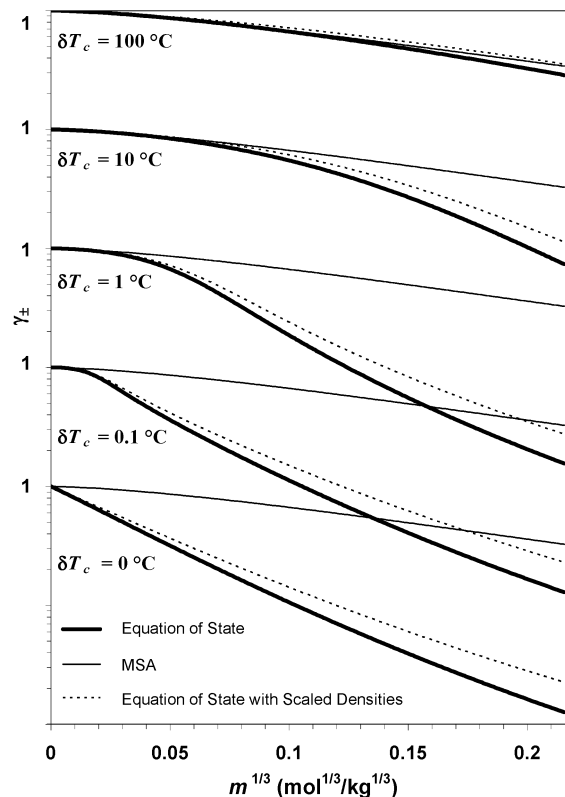


**Figure 1.** Mean ionic activity coefficient of aqueous NaCl solutions at the critical density and various distances away from the critical temperature. For each curve,  $\gamma_{\pm}$  is plotted on a log scale with  $\gamma_{\pm} = 1$  at  $m = 0$  and major tick marks decreasing in powers of 10 from top to bottom.

isotherm–isobar. However, the range of validity of the Debye–Hückel limiting law decreases as the critical point is approached. On the critical isotherm–isobar, the equation of state leads to the  $x^{1/3}$  limiting law. As the distance from the critical point is increased, the range of validity of the Debye–Hückel limiting law increases. At higher concentrations, vestiges of the  $x^{1/3}$  limiting law are clearly evident even at state points quite far from the critical point.

Figures 3–6 show the ratio of the equation-of-state activity coefficient to the MSA activity coefficient ( $\gamma_{\pm}/\gamma_{\pm}^{\text{MSA}}$ ) near the critical point. The departures of this ratio from unity are very large at 0.01  $m$  and increase with increasing molality. At 0.01  $m$ ,  $\gamma_{\pm}$  calculated from the equation of state is less than 50% of  $\gamma_{\pm}^{\text{MSA}}$  at  $\delta \rho_c = 0$  with  $\delta T_c < 25$  K and at  $\delta T_c = 0$  with  $\delta \rho_c < 80$  kg/m<sup>3</sup>. Effects this large are found only much closer to the critical point at 0.0001  $m$ . To explore the reasons for this very large effect, we repeated the calculation after removing the Born solvation term from our equation of state. The same qualitative behavior was observed, but the magnitude of the anomalous effect was much smaller. Large vestiges of the  $x^{1/3}$  law were visible only extremely close to the critical temperature and density. The effect should be very large for all aqueous electrolyte solutions because they have large contributions from the Born term near the critical point. The expression for the Born contribution to the activity coefficient is given by

$$\ln \gamma_i^{\text{Born}}(T, P) = \frac{N_a e^2 Z_i^2}{4\pi \epsilon_0 \sigma_i} \left( \frac{1}{\epsilon} - \frac{1}{\epsilon_{\text{infinite dilution}}} \right) \quad (23)$$

The values of the ion diameters,  $\sigma_i$ , in eq 23 were obtained from the temperature correlation of eq 17 and represent the diameters

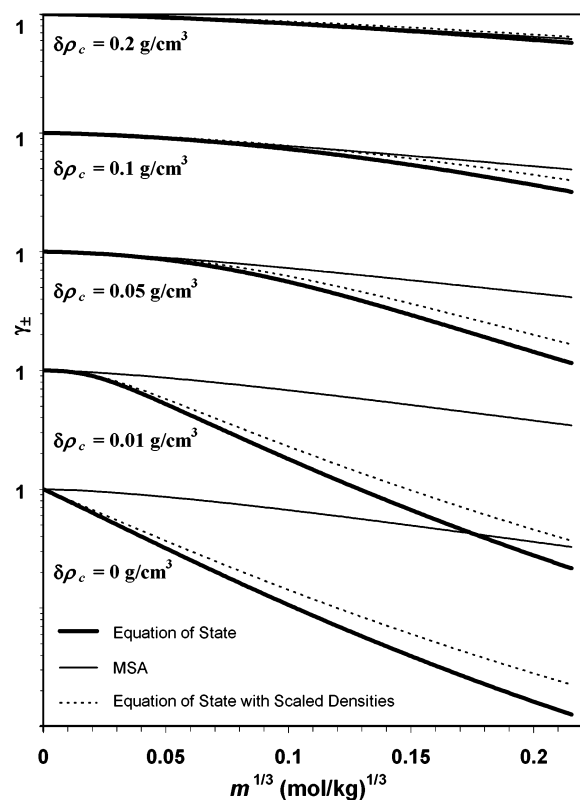


**Figure 2.** Mean ionic activity coefficient of aqueous NaCl solutions at the critical temperature and various distances away from the critical density. For each curve,  $\gamma_{\pm}$  is plotted on a log scale with  $\gamma_{\pm} = 1$  at  $m = 0$  and major tick marks decreasing in powers of 10 from top to bottom.

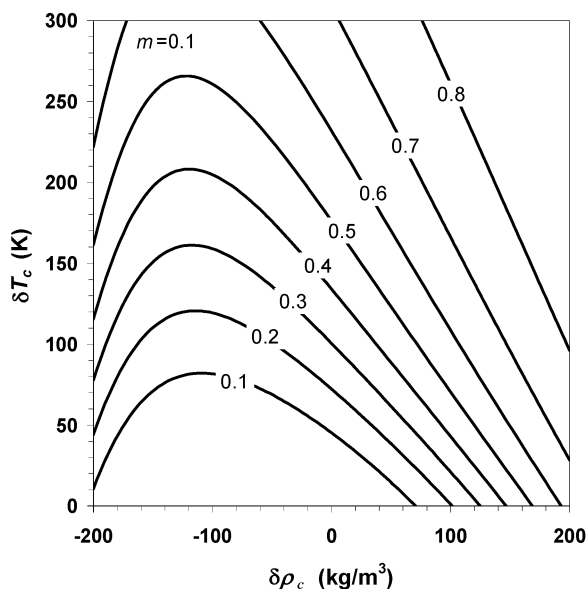


**Figure 3.** Contour plot of  $\gamma_{\pm}/\gamma_{\text{MSA}}$  of aqueous NaCl solutions as a function of  $\delta T_c$  and  $\delta\rho_c$  for  $m = 0.1$ .

of the hydrated ions. These diameters are larger than the crystal diameters of the pure ions and, when used in the Born equation, give more accurate predictions of the free energies of hydration. The dielectric constant used in our calculations was that of pure water at the temperature and water concentration of the system. For dilute aqueous solutions at ambient conditions, the difference between this dielectric constant and that of pure water at infinite dilution water concentration and the same temperature is small. Close to the critical point, though, this difference will be

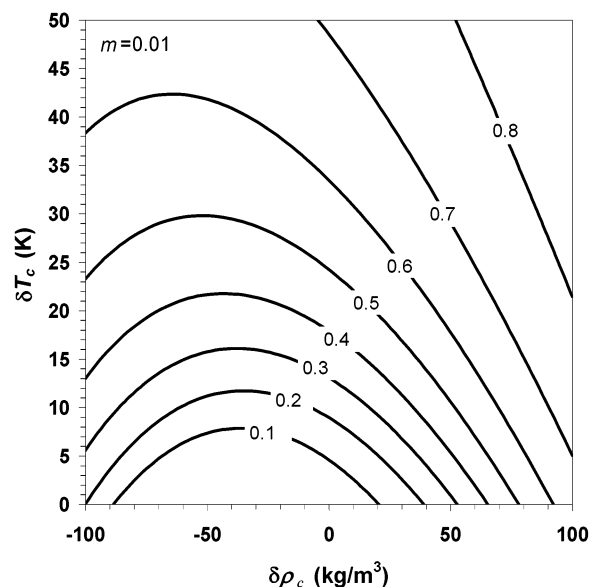


**Figure 4.** Contour plot of  $\gamma_{\pm}/\gamma_{\text{MSA}}$  of aqueous NaCl solutions as a function of  $\delta T_c$  and  $\delta\rho_c$  for  $m = 0.01$ .

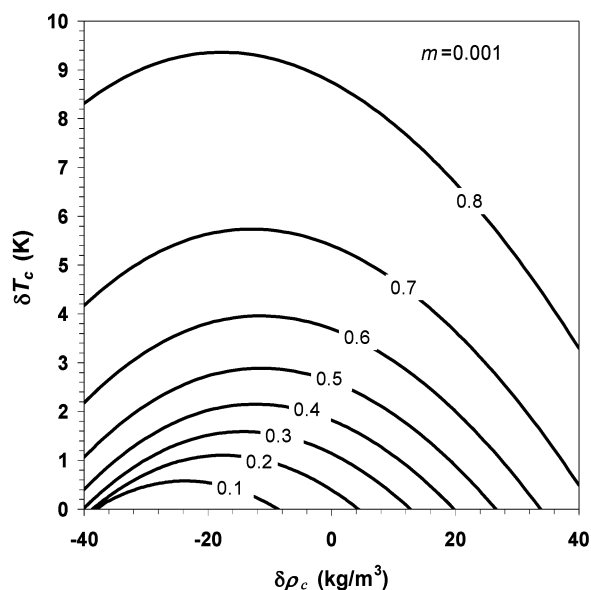


**Figure 5.** Contour plot of  $\gamma_{\pm}/\gamma_{\text{MSA}}$  of aqueous NaCl solutions as a function of  $\delta T_c$  and  $\delta\rho_c$  for  $m = 0.001$ .

significant—because of electrostriction, there is a large variation of density with salt concentration in near-critical solutions. This effect is illustrated in Figures 7 and 8 in which the density and dielectric constant of water calculated using our model are plotted as functions of NaCl molality at the critical point. The large anomalies in the activity coefficients of electrolyte solutions near the critical point of water can thus be attributed to the large magnitudes of the Born term resulting from the significant density changes with salt concentration in this region.

Because the equation of state underestimates the critical density of water (Table 1), the dielectric constant at the critical point predicted by the equation of state is less than that of real water at the critical point. To examine the consequences of this, we repeated our calculations with densities (used to calculate the dielectric constant) that were scaled by the ratio of the actual critical density of water to the equation-of-state critical density. The results are indicated by the dashed lines in Figures 1 and 2, which can be compared with the results of the previous calculation. The effect of scaling the densities is that the



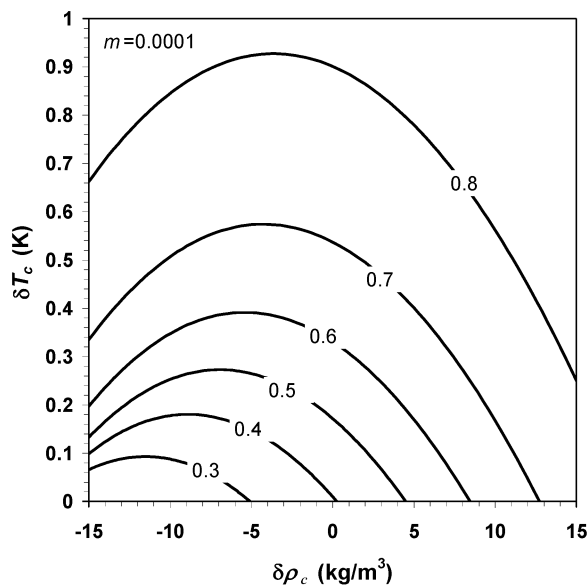


**Figure 6.** Contour plot of  $\gamma_{\pm}/\gamma_{\text{MSA}}$  of aqueous NaCl solutions as a function of  $\delta T_c$  and  $\delta \rho_c$  for  $m = 0.0001$ .

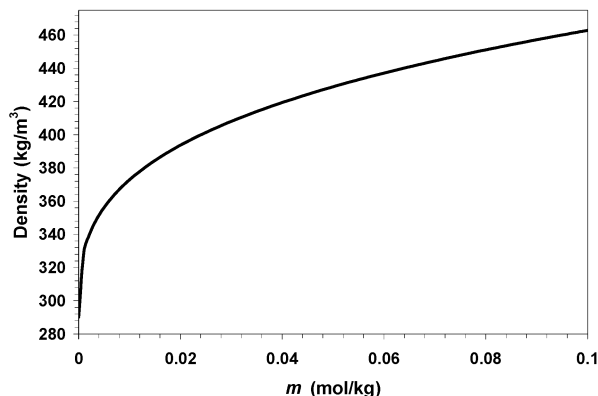


**Figure 7.** Density of water as a function of NaCl molality at the critical  $T$  and  $P$  of pure water.

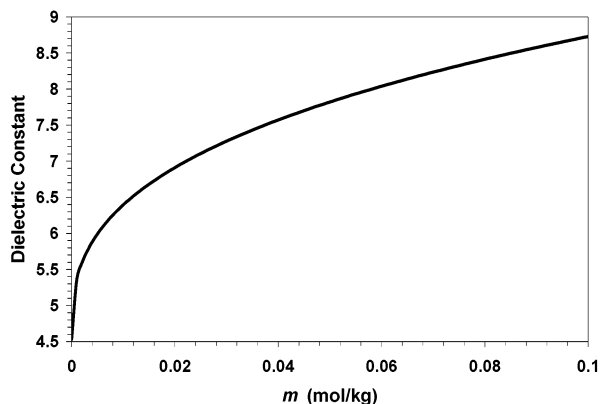


**Figure 8.** Dielectric constant of water as a function of NaCl molality at the critical  $T$  and  $P$  of pure water.

calculated activity coefficients are slightly larger and the magnitude of the effect given by eq 23 is smaller. Thus, with scaled densities, the large observed electrostriction effect is slightly decreased. Still, large anomalies in the activity coefficients near the critical point remain.

We also repeated the calculations along a path starting at the critical point and keeping the volume and the activity of water constant as the concentration of NaCl increased. This is the McMillan–Mayer standard state. The result was that the

activities were very much the same as on the isotherm–isobar, so the differences between the two states are small.

The present model for activity coefficients cannot be directly tested because there are no experimental measurements close to the critical point of water. However, Gruskiewicz and Wood<sup>14</sup> measured conductances of NaCl solutions very close to the critical point (649.6 K and 323.7 kg/m<sup>3</sup>). Activity coefficients affect the degree of association of NaCl, particularly at the highest concentrations, and this changes the conductance. The results of refitting the conductance data of Gruskiewicz and Wood near the critical point were surprising. Our activity coefficient model did not fit experimental data at the highest concentrations as well as the MSA model. However, if the two highest concentration points were omitted, then both models gave the same values of  $\Lambda^0$  and  $\log K$  as the published values within their 95% confidence limits, indicating that the published values of  $\Lambda^0$  and  $\log K$  are accurate. One possible explanation for the failure to fit the high-concentration data is that the present equation overestimates the change in dielectric constant with added salt. An activity coefficient model that leads to values between the MSA model and the present equation would fit the highest concentration because the equivalent conductance calculated at this point with  $\gamma_{\text{MSA}}$  is low by 170 S cm<sup>2</sup>/mol and it is high by 350 S cm<sup>2</sup>/mol with  $\gamma_{\pm}$  of the present equation.

## Conclusions

The model of Myers et al.<sup>15</sup> was not parametrized at or near the critical point; it is a classical model, so its accuracy will be only semiquantitative near the critical point. However, the model confirms the qualitative prediction of Levelt Sengers et al.<sup>1</sup> that the range of validity of the Debye–Hückel limiting law is diminished as the critical point is approached and that vestiges of the  $x^{1/3}$  limiting law increasingly dominate the activity coefficients at higher concentrations. For ions we find very large vestiges of the critical point anomalies quite far from the critical point, and these anomalies increase with increasing concentration. The large magnitude of the anomalies for ions in the Myers et al. model is due to the very large change in the solvent dielectric constant with the addition of ions. Refitting of the conductance data of Gruskiewicz and Wood<sup>14</sup> near the critical point indicates that their reported values of  $\Lambda^0$  and  $\log K$  are accurate and that the equation of Myers et al. may overestimate the critical-point anomalies. Scaling the densities in the equation of state by the ratio of the actual to the calculated critical density of water slightly decreases the large apparent electrostriction effect.

The anomalies shown here should be kept in mind when dealing with systems with near-critical and supercritical solutions of electrolytes. Although we have shown results only for aqueous NaCl solutions, we expect that other ionic solutions will have the same qualitative behavior near the critical point because the electrostriction effects will be similar.

**Acknowledgment.** Financial support for this research was provided by the National Science Foundation (CTS-0083709) and the Department of Energy (DE-FG02-85ER-13436 and DE-FG02-89ER-14080).

## References and Notes

- (1) Levelt Sengers, J. M. H.; Harvey, A. H.; Crovetto, R.; Gallagher, J. S. *Fluid Phase Equilib.* **1992**, *81*, 85.
- (2) Levelt Sengers, J. M. H.; Everhart, C. M.; Morrison, G.; Pitzer, K. S. *Chem. Eng. Commun.* **1986**, *47*, 315.
- (3) Levelt Sengers, J. M. H. In *Supercritical Fluid Technology: Reviews in Modern Theory and Applications*; Bruno, T. J., Ely, J. F., Eds.; CRC Press: Boca Raton, FL, 1992; Chapter 1.

- (4) Debye, P.; Hückel, E. *Phys. Z* **1923**, 24, 185.
- (5) Levelt Sengers, J. M. H. *Int. J. Thermophys.* **1990**, 11, 399.
- (6) Benson, S. W.; Copeland, C. S.; Pearson, D. *J. Chem. Phys.* **1953**, 21, 2208.
- (7) Krichevskii, I. R. *Russ. J. Phys. Chem.* **1967**, 41, 1332.
- (8) Rozen, A. M. *Russ. J. Phys. Chem.* **1976**, 50, 837.
- (9) Wheeler, J. C. *Ber. Bunsen-Ges. Phys. Chem.* **1972**, 76, 308.
- (10) Busey, R. H.; Holmes, H. F.; Mesmer, R. E. *J. Chem. Thermodyn.* **1984**, 16, 343.
- (11) Chang, R. F.; Morrison, G.; Levelt Sengers, J. M. H. *J. Phys. Chem.* **1984**, 88, 3389.
- (12) Biggerstaff, D. R.; Wood, R. H. *J. Phys. Chem.* **1988**, 92, 1988.
- (13) Crovetto, R.; Wood, R. H.; Majer, V. *J. Chem. Thermodyn.* **1991**, 23, 1139.
- (14) Gruszkiewicz, M. S.; Wood, R. H. *J. Phys. Chem. B* **1997**, 101, 6549.
- (15) Myers, J. A.; Sandler, S. I.; Wood, R. H. *Ind. Eng. Chem. Res.* **2002**, 41, 3282.
- (16) Uematsu, M.; Franck, E. U. *J. Phys. Chem. Ref. Data* **1980**, 9, 1291.
- (17) Fernandez, D. P.; Goodwin, A. R. H.; Lemmon, E. W.; Levelt Sengers, J. M. H.; Williams, R. C. *J. Phys. Chem. Ref. Data* **1997**, 26, 1125.
- (18) Harvey, A. H.; Copeman, T. W.; Prausnitz, J. M. *J. Phys. Chem.* **1988**, 92, 6432.
- (19) Wagner, W.; Pruss, A. *J. Phys. Chem. Ref. Data* **2002**, 2, 387.
- (20) Chang, R. F.; Levelt Sengers, J. M. H. *J. Phys. Chem.* **1986**, 90, 5921.